Impact of Lithium-Ion Ordering on Surface Electronic States of Li_xCoO_2

K. Iwaya,[1,2] T. Ogawa,[3] T. Minato,[4,5] K. Miyoshi,[6] J. Takeuchi,[6] A. Kuwabara,[3] H. Moriwake,[3] Y. Kim,[4] and T. Hitosugi[1]

[1]*Advanced Institute for Materials Research, Tohoku University, Sendai 980-8577, Japan*
[2]*Center for Emergent Matter Science, RIKEN, Wako, Saitama 351-0198, Japan*
[3]*Japan Fine Ceramic Center, Nagoya 456-8587, Japan*
[4]*Surface and Interface Science Laboratory, RIKEN, Wako 351-0198, Japan*
[5]*International Advanced Research and Education Organization, Tohoku University, Sendai 980-8578, Japan*
[6]*Department of Material Science, Shimane University, Matsue 690-8504, Japan*

(Received 16 July 2013; published 18 September 2013)

Li_xCoO_2 exhibits intriguing electronic properties due to a strong electron correlation and complex interplay between Co and Li ions. However, fundamental understanding of the nanoscale distribution of Li ions and its effect on the electronic properties remains unclear. We use scanning tunneling microscopy and density functional theory to elucidate the degree of Li_xCoO_2 surface electronic state modification that can be achieved by Li ordering. The surface Li ions are highly mobile and preferentially form a (1×1) hexagonal lattice, whereas the surface CoO_2 layer shows metallic and insulating phases, indicating the coexistence of ordered and disordered Li ions in the subsurface layer. These results provide evidence of novel electronic properties produced by spatially inhomogeneous Li-ordering patterns.

DOI: 10.1103/PhysRevLett.111.126104 PACS numbers: 68.47.Gh, 68.37.Ef, 71.15.Mb, 71.27.+a

Rechargeable lithium batteries are ubiquitous in modern society. However, despite their widespread use (from portable electronics to hybrid-electric vehicles), a microscopic understanding of the battery operation, for example, the atomic-scale process of Li intercalation/deintercalation at the electrode-electrolyte interface, remains unclear. To further improve battery performance, such fundamental knowledge requires experimental investigation [1]. The atomic-scale surface structure and its electronic states of electrode materials such as $LiCoO_2$ are particularly important because they profoundly affect the efficiency of electrochemical reaction. Moreover, recent trends to improve the electrochemical performance are to utilize the nanostructure effect, expecting its higher surface area [2,3] and surface modification such as metal-oxide coating [4]. These effects also involve the electrode material surfaces, and thus demands for understanding the atomic-scale surface properties have been further increasing. While theoretical studies of such surfaces were previously reported by assuming ideal surface terminations expected from the crystal structure [5,6], experimental understanding of these properties remains elusive.

Layered $LiCoO_2$, the widely used cathode material in commercial Li-ion batteries, has also attracted considerable interest in condensed-matter physics because this material is prototypical to study the interplay between electron correlation and order or disorder due to highly mobile Li ions [7]. By deintercalating Li, Co ions are in the mixed-valence state having spins of $S = 0$ (Co^{3+}) and $S = 1/2$ (Co^{4+}) and form the two-dimensional triangular lattice, which produces the geometrical spin frustration [8]. In addition, various orderings of Li ions and vacancies are proposed depending on Li content x [9–11]. Owing to these situations, Li_xCoO_2 exhibits a rich electronic phase diagram as a function of x [12,13].

Whereas real-space imaging of Li-ion diffusion in $LiCoO_2$ has been previously reported, spatial resolution of these measurements is still limited to submicron grain size [14,15]. High-resolution transmission electron microscopy can image Li-ion columns but cannot resolve individual Li ions [16–18] and has difficulties in probing the electronic information. Scanning tunneling microscopy (STM) is ideal for this purpose due to its high spatial resolution and spectroscopic capability.

$Li_{0.66}CoO_2$ (i.e., $Co^{3+}/Co^{4+} = 2{:}1$), which shows anomalous transport and magnetic properties at $T \sim 155$ K [19], was chosen in this study. The details about sample preparation and characterization are described in Ref. [19]. To perform STM measurements, we prepare a well-defined sample surface by cleaving $Li_{0.66}CoO_2$ single crystals along the ab plane at $T \sim 90$ K in ultrahigh vacuum conditions. Since the weakest bond is located between adjacent CoO_2 layers [Fig. 1(a)], the exposed surface atom after cleaving is believed to be either Li or the topmost oxygen of the CoO_2 layer. The cleaved surfaces showed steps corresponding to multiples of $1/3$ unit cell height $(c/3)$, with $c = 1.43$ nm, as expected from the crystal structure. All of the STM measurements were performed at $T \sim 5$ K.

Figure 1(b) displays a STM image of $Li_{0.66}CoO_2$ at a sample bias voltage $V_s = -1.0$ V, exhibiting a hexagonal atomic lattice constant of ~0.3 nm. This is in good agreement with a lattice constant of $LiCoO_2$ ($a_0 = 0.28$ nm). A differential conductance (dI/dV) spectrum taken at this surface showed an insulating gap [Fig. 1(c)], which is inconsistent with the metallic behavior observed in bulk

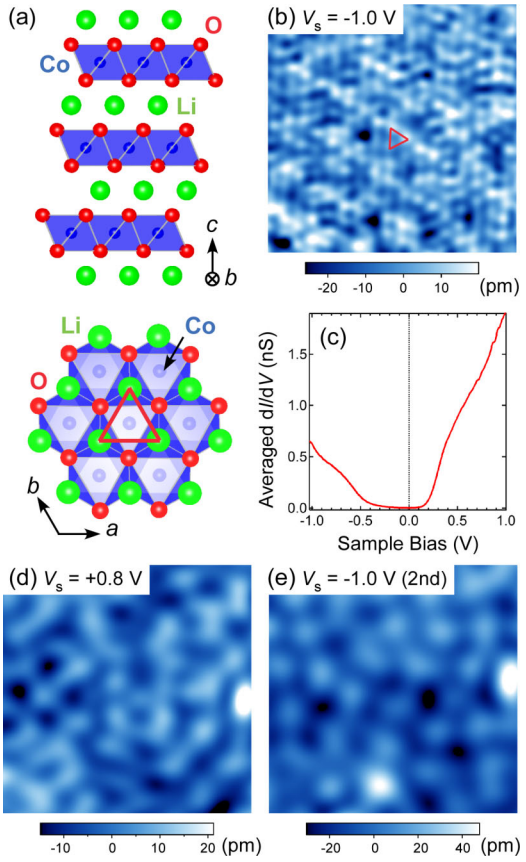

FIG. 1 (color online). (a) Crystal structure of the layered $LiCoO_2$ (α-$NaFeO_2$ structure, $R\bar{3}m$). Bottom: ab plane. A triangle consisting of surface Li atoms is shown. (b) Constant-current STM image of a $Li_{0.66}CoO_2$ single crystal measured at 5 K, showing hexagonal lattice of Li ions at the surface; 4.8×4.8 nm^2, sample bias voltage $V_s = -1.0$ V, and tunneling current $I_t = 0.2$ nA. The atomic spacing (~ 0.3 nm) is consistent with the Li-Li distance shown as a triangle. (c) Averaged differential conductance dI/dV spectrum taken at surface Li ions in (b). Set point: $I_t = 0.2$ nA, $V_s = -1.0$ V. (d) STM image at $V_s = +0.8$ V measured at the same location as in (b). (e) STM image at the same location as in (b), subsequently taken after (d) at $V_s = -1.0$ V.

transport measurements [19]. We next examined V_s dependence of the STM image at the same location. Figure 1(d) is the STM image at $V_s = +0.8$ V taken just after imaging at $V_s = -1.0$ V [Fig. 1(b)]. At $V_s = +0.8$ V, no hexagonal lattice was observed and instead randomly distributed protrusions were visualized. Subsequently, we imaged the same location at $V_s = -1.0$ V again and found randomly distributed protrusions rather than the originally observed hexagonal lattice [Fig. 1(e)]. Notably, we identified the (1×1) hexagonal lattice in the surrounding area. It is thus likely that the hexagonal lattice can be attributed to Li ions at the surface and removed by electric fields between STM tip and surface, whereas the random protrusions appearing after bias-polarity change can be attributed to the underlying CoO_2 layer. We also found that depending on subtle changes in the tip-surface interaction, STM images showed hexagonal lattice or noisy features even when taken at the same location [Supplemental Material [20]], strengthening the idea that the hexagonal lattice is formed by Li ions at the surface.

The formation of (1×1) hexagonal lattice of Li ions provides valuable information about the electronic configuration of subsurface Co ions. It is known that to stabilize polar surfaces, Li_xCoO_2 surfaces need to provide charge compensation (i.e., a valence change of Co ion near the surface) [5,21]. For example, in the case that the surface of $LiCoO_2$ is terminated with Li layer, $1/2$ monolayer of Li ions is reasonable to satisfy this global charge balance without the valence change of Co ions. In this situation, all the subsurface Co ions are in the form of Co^{3+}. Thus, to realize the observed (1×1) hexagonal Li-ion ordering at the surface, the valence change of subsurface Co ions is required. Since excess Li ions exist at the (1×1) hexagonal surface, some of the subsurface Co ions need to be reduced to Co^{2+}, which corresponds to n-type doping into the subsurface CoO_2 layer [Supplemental Material [21]]. This picture is consistent with the n-type behavior observed in the dI/dV spectrum [Fig. 1(c)], supporting the existence of Co^{2+} ions near the surface previously reported in $LiCoO_2$ nanoparticles [2].

We observed the hexagonal Li ion lattice only in a small fraction of the surface, possibly because of cleaving. Most imaged areas showed a CoO_2 layer, at which two distinct structures were found: ordered and disordered structure. First, we discuss the ordered structure. Figure 2(a) shows a representative STM image at $V_s = -0.6$ V, exhibiting a (3×3) hexagonal lattice. In bulk $Li_{0.66}CoO_2$, we naturally expect that Co^{4+} ions distribute to form a hexagonal lattice with a spacing of $\sqrt{3}a_0$, as theoretically discussed [22]. However, this spacing is substantially smaller than the observed $3a_0$. Remarkably, by changing the polarity of V_s, the contrast of the image was reversed [Figs. 2(b) and 2(c)]. In addition, dI/dV spectra measured at this area showed metallic behavior [Fig. 2(d)], different from that of the surface covered by Li [Fig. 1(c)].

The contrast reversal with V_s polarity is a typical signature of charge ordering, seen in perovskite manganites [23]. In analogy with the manganite, we can assume that the (3×3) hexagonal lattice originates from the ordering of Co^{4+} or Co^{3+} ions, which corresponds to $Co^{3+}/Co^{4+} = 8{:}1$ ($x = 0.89$) or $1{:}8$ ($x = 0.11$), respectively. In the case of $x = 0.89$, previous bulk transport measurements reported a semiconducting behavior [19], which is inconsistent with the substantial density of state (DOS) observed at Fermi energy in the tunneling spectra. In the case of $x = 0.11$, such a large discrepancy from the bulk content ($x = 0.66$) is unlikely.

To elucidate the observed structure, we performed spin polarized density functional theory (DFT) + U calculations [Supplemental Material [24]]. The surface structure

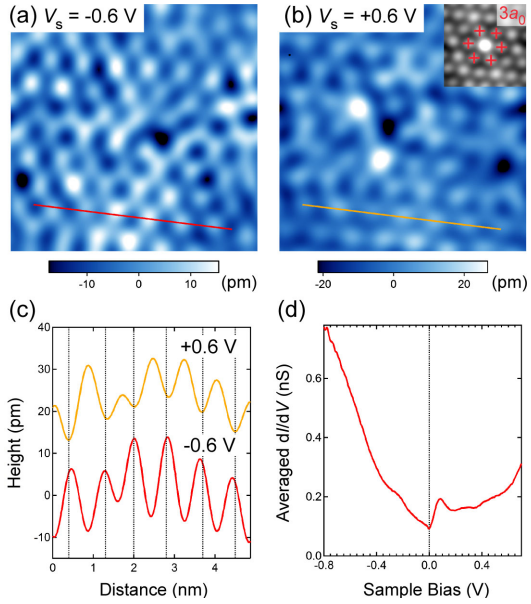

FIG. 2 (color online). [(a) and (b)] Bias-dependent STM image of $Li_{0.66}CoO_2$ at $V_s = -0.6$ and $+0.6$ V, showing (3×3) structures, respectively; 6×6 nm^2, $I_t = 0.3$ nA. The autocorrelation image of (b) is shown in the inset. (c) Comparison of line profile of the STM image at -0.6 and $+0.6$ V in (a) and (b). For clarity, the line profile at $+0.6$ V is shifted vertically. (d) Averaged dI/dV spectrum taken in (a). Set point: $I_t = 0.3$ nA, $V_s = -0.8$ V.

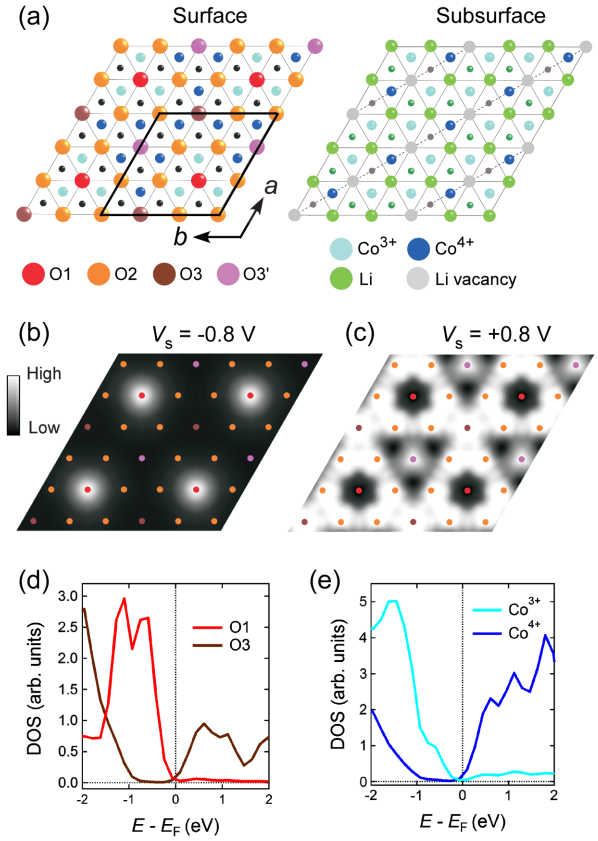

FIG. 3 (color online). (a) Schematic structure of the (3×3) ordering at $Li_{0.66}CoO_2$ surface. Left: surface structure, right: subsurface structure. The surface is terminated with CoO_2 layer, in which $Co^{3+}/Co^{4+} = 1{:}2$ is realized due to the charge balance effect. The surface oxygen atom O1 lies among three adjacent Co^{3+} ions, O2 is surrounded by one Co^{3+} and two Co^{4+} ions, and O3 lies among adjacent three Co^{4+} ions. O3′ is also surrounded by three Co^{4+} ions but has an outer atomic arrangement different from that of O3. Oxygen atoms located below Co ions are illustrated as smaller circles. The (3×3) unit cell is shown as a thick solid line. In the subsurface layer (right), Li vacancies and Co^{4+} ions are introduced to satisfy $x = 0.66$ (i.e., $Co^{3+}/Co^{4+} = 2{:}1$) and placed to form the $(\sqrt{3} \times \sqrt{3})R30°$ structure. Li ions and vacancies located below this layer are illustrated as smaller circles. [(b) and (c)] Simulated integrated DOS images from spin-polarized DFT calculations at $V_s = -0.8$ and $+0.8$ V, respectively. The position of each surface oxygen atom is indicated using the same color as in (a). (d) Simulated partial DOSs of surface oxygen atoms O1 and O3 in (a). Majority and minority spin components are added together. (e) Simulated partial DOSs of Co^{3+} and Co^{4+} ions in (a). Majority and minority spin components are added together.

that can qualitatively reproduce both the STM images and metallic spectrum is shown in Fig. 3(a). We assumed $Co^{3+}/Co^{4+} = 2{:}1$ in bulk and determined the surface Co^{3+}/Co^{4+} ratio based on the total charge balance effect [5]. Since the surface is terminated with CoO_2 layers, Li ions exist only in the subsurface layer. In this case, the Co^{3+}/Co^{4+} ratio at the surface is expected to be $Co^{3+}/Co^{4+} = 1{:}2$, different from that of the bulk [Supplemental Material [21]]. In the bulk, Li vacancies and Co^{4+} form a $(\sqrt{3} \times \sqrt{3})R30°$ structure, as expected from short-ranged repulsive interactions [Fig. 3(a), right] [22]. We found that to reproduce the (3×3) structure, three surface Co^{3+} ions need to be located at the nearest sites in the unit cell, as illustrated in Fig. 3(a), left. In this model, there exist three different surface oxygen atoms depending on the surrounding environments: O1, which is surrounded by three adjacent Co^{3+} ions, O2, which is surrounded by one Co^{3+} and two Co^{4+} ions, and O3, which is surrounded by three adjacent Co^{4+} ions [Fig. 3(a), left]. DFT simulations reveal that STM images mainly consist of surface oxygen atoms in both filled and empty states. In the filled states, the O1 atoms are most enhanced, indicating substantial hybridization with occupied t_{2g} orbital states of the surrounding Co^{3+} ions [Fig. 3(b)], while in the empty states, the O1 atoms are strongly suppressed and instead the O3 atoms are most enhanced, reflecting significant hybridization with unoccupied d-orbital states of the neighboring Co^{4+} ions [Fig. 3(c)].

The contrast reversal can be readily identified in simulated partial DOS of O1 and O3 [Fig. 3(d)]. In addition, the energy gap becomes almost negligibly small [Fig. 3(e)], which is qualitatively consistent with the observed dI/dV spectrum. For comparison, we also calculated the partial DOS in a different ordering pattern of Co^{3+} and Co^{4+} ions, in which each Co^{3+} ion is evenly distributed to form a (3×3)

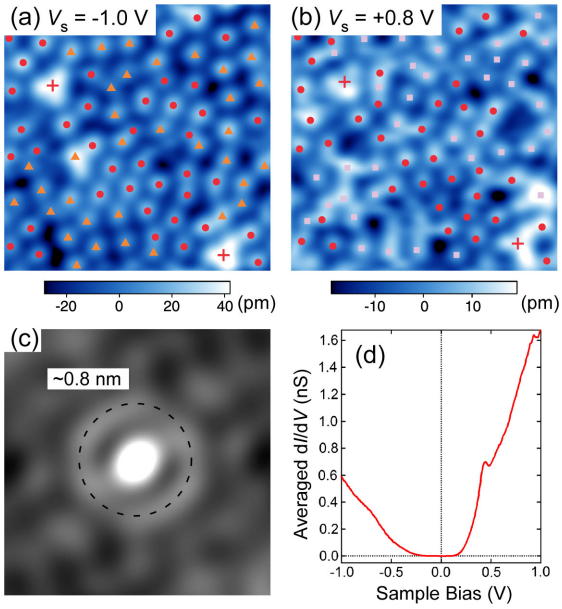

FIG. 4 (color online). [(a) and (b)] Bias-dependent STM images of $Li_{0.66}CoO_2$ at $V_s = -1.0$ and $+0.8$ V, showing disordered structures, respectively. Both images were taken at the same position; 7×7 nm^2, $I_t = 0.3$ nA. There exist three different protrusions, which appear only at -1.0 V (triangles) and $+0.8$ V (squares) and at both voltages (circles). To compare between these two images, the identical positions are indicated as crosses. (c) Autocorrelation image of (a). (d) Averaged dI/dV spectrum taken in (a). Set point: $I_t = 0.2$ nA, $V_s = -1.0$ V.

structure due to the short-ranged repulsive interactions [Supplemental Material [25]]. In this case, simulated DOS shows a large energy gap, as expected from charge ordering. This indicates that the ordering pattern of Co ions plays a crucial role for determining the surface electronic states as well as that of Li.

Another distinct feature observed in the CoO_2 layer is a disordered structure [Fig. 4(a)]. By changing V_s polarity, we found three different types of protrusions, which appear only in positive V_s, only in negative V_s, and in both V_s polarities [Figs. 4(a) and 4(b)]. They are possibly associated with the three different surface oxygens, O1, O2, and O3, discussed in Fig. 3(a). The autocorrelations of these images show an almost isotropic feature, indicating no preferential ordering [Fig. 4(c)]. The dI/dV spectrum taken at this disordered surface exhibits an insulating gap [Fig. 4(d)], similar to that on the (1×1) surface Li ions [Fig. 1(c)], implying a different concentration of Li ions from that of the metallic (ordered) area. The insulating gap could be observed when the subsurface Li sites were almost fully occupied with Li ions. However, in this case, we would expect a more ordered STM image than that of the disordered structure. Another possible scenario is that the insulating gap might arise from the random distribution of Li ions at the subsurface intercalation sites. In conventional doped semiconductors, the metal-insulator transition can be induced by Anderson localization, where conduction electrons are so scattered by randomly distributed impurity atoms that they become localized [26]. We propose that a similar situation is realized at this surface.

These results clearly demonstrate that Li_xCoO_2 surface states are heterogeneous due to the spatially different concentration and ordering pattern of Li ions. Although the effect of spatially inhomogeneous Li concentration on the electronic properties has long been discussed [27], we further reveal that in addition to this effect, the ordering pattern of Li ions can greatly modify the electronic states of the Li_xCoO_2 surface. In the related material Na_xCoO_2, similar electronic modifications due to the Na ordering were indeed observed using diffraction techniques [28]. Our results represent direct imaging of such ordering effects in Li_xCoO_2. Considering highly mobile Li ions, other ordering patterns, as theoretically predicted [10] might form locally on the same surface, and such orderings are possibly formed in bulk as well.

The observation of these distinctive electronic states, attributed to the ordering pattern of Li and Co ions, can help elucidate unresolved results in previous studies. Previous magnetization measurements for $Li_{0.66}CoO_2$ single crystals taken from the same batch used in this study showed a clear cooling-rate dependence below 130 K, where Li ions stop diffusing [19]. To understand this behavior, it was suggested that the Li-ordering pattern would depend on the cooling rate and also modify the ordering of Co^{3+}/Co^{4+} so that the total magnetization originated from Co ions could be strongly dependent on the cooling rate [19]. Our results support this scenario, providing strong evidence that the Li-ordering pattern plays a decisive role in determining the ordering of Co ions. In addition, the coexistence of metallic and insulating regions found in this study is consistent with the picture of the partial carrier localization explaining unexpectedly small transition entropy at the anomaly ($T \sim 155$ K) in previous transport measurements [19]. The (1×1) hexagonal surface Li ions observed in this study account for the existence of Co^{2+} ions in the subsurface layers, which was previously doubtful because the deintercalation of Li ions produces Co^{4+} rather than Co^{2+} [2,6]. The removal of surface Li ions by the changing of local electric fields demonstrated in this study may be potentially used to control spatial Li distribution with much higher precision than that of the previous results [15]. In terms of the battery cathode material, the important role of surface is common to other lithium metal oxides such as $LiMn_2O_4$, $Li_4Ti_5O_{12}$, and $LiFePO_4$ [4,6,29,30]. Consequently, atomic-scale understanding of interfacial structures existent in Li-ion batteries should be developed to enhance the electrochemical properties and also to further extract the potential capabilities of the lithium metal oxides at the nanoscale.

We thank P. Han, K. Akagi, and S. Shiraki for valuable discussions. This work was supported by the World

Premier Research Institute Initiative promoted by the Ministry of Education, Culture, Sports, Science and Technology (MEXT) of Japan, and by a Grant-in-Aid for Scientific Research from MEXT.

[1] J.-M. Tarascon and M. Armand, Nature (London) **414**, 359 (2001).
[2] M. Okubo, E. Hosono, J. Kim, M. Enomoto, N. Kojima, T. Kudo, H. Zhou, and I. Honma, J. Am. Chem. Soc. **129**, 7444 (2007).
[3] A. S. Arico, P. Bruce, B. Scrosati, J.-M. Tarascon, and W. Van Schalkwijk, Nat. Mater. **4**, 366 (2005).
[4] S.-T. Myung, K. Amine, and Y.-K. Sun, J. Mater. Chem. **20**, 7074 (2010).
[5] D. Kramer and G. Ceder, Chem. Mater. **21**, 3799 (2009).
[6] D. Qian, Y. Hinuma, H. Chen, L.-S. Du, K. J. Carroll, and G. Ceder, J. Am. Chem. Soc. **134**, 6096 (2012).
[7] C. A. Marianetti, G. Kotliar, and G. Ceder, Nat. Mater. **3**, 627 (2004).
[8] J. Sugiyama, H. Nozaki, J. H. Brewer, E. J. Ansaldo, G. D. Morris, and C. Delmas, Phys. Rev. B **72**, 144424 (2005).
[9] J. N. Reimers and J. R. Dahn, J. Electrochem. Soc. **139**, 2091 (1992).
[10] C. Wolverton and A. Zunger, Phys. Rev. Lett. **81**, 606 (1998).
[11] Y. Shao-Horn, S. Levasseur, F. Weill, and C. Delmas, J. Electrochem. Soc. **150**, A366 (2003).
[12] T. Motohashi, T. Ono, Y. Sugimoto, Y. Masubuchi, S. Kikkawa, R. Kanno, M. Karppinen, and H. Yamauchi, Phys. Rev. B **80**, 165114 (2009).
[13] T. Y. Ou-Yang, F.-T. Huang, G. J. Shu, W. L. Lee, M.-W. Chu, H. L. Liu, and F. C. Chou, Phys. Rev. B **85**, 035120 (2012).
[14] N. Balke, S. Kalnaus, N. J. Dudney, C. Daniel, S. Jesse, and S. V. Kalinin, Nano Lett. **12**, 3399 (2012).
[15] N. Balke, S. Jesse, A. N. Morozovska, E. Eliseev, D. W. Chung, Y. Kim, L. Adamczyk, R. E. Garcia, N. Dudney, and S. V. Kalinin, Nat. Nanotechnol. **5**, 749 (2010).
[16] Y. Shao-Horn, L. Croguennec, C. Delmas, E. C. Nelson, and M. A. O'keefe, Nat. Mater. **2**, 464 (2003).
[17] R. Huang, T. Hitosugi, S. D. Findlay, C. A. Fisher, Y. H. Ikuhara, H. Moriwake, H. Oki, and Y. Ikuhara, Appl. Phys. Lett. **98**, 051913 (2011).
[18] H. Moriwake, A. Kuwabara, C. A. J. Fisher, R. Huang, T. Hitosugi, Y. H. Ikuhara, H. Oki, and Y. Ikuhara, Adv. Mater. **25**, 618 (2013).
[19] K. Miyoshi, C. Iwai, H. Kondo, M. Miura, S. Nishigori, and J. Takeuchi, Phys. Rev. B **82**, 075113 (2010).
[20] See the Supplemental Material at http://link.aps.org/supplemental/10.1103/PhysRevLett.111.126104 for imaging of the surface Li ions.
[21] See the Supplemental Material at http://link.aps.org/supplemental/10.1103/PhysRevLett.111.126104 for the charge balance at Li_xCoO_2 surfaces.
[22] M. E. Arroyo y de Dompablo, C. Marianetti, A. Van der Ven, and G. Ceder, Phys. Rev. B **63**, 144107 (2001).
[23] J. X. Ma, D. T. Gillaspie, E. W. Plummer, and J. Shen, Phys. Rev. Lett. **95**, 237210 (2005).
[24] See the Supplemental Material at http://link.aps.org/supplemental/10.1103/PhysRevLett.111.126104 for the detail about theoretical simulations.
[25] See the Supplemental Material at http://link.aps.org/supplemental/10.1103/PhysRevLett.111.126104 for another possible Co ordering pattern.
[26] P. P. Edwards, C. N. R. Rao, and N. F. Mott, *Metal-insulator Transitions Revisited* (Taylor & Francis, London, UK; Bristol, PA, USA, 1995).
[27] M. Menetrier, I. Saadoune, S. Levasseur, and C. Delmas, J. Mater. Chem. **9**, 1135 (1999).
[28] M. Roger, D. J. P. Morris, D. A. Tennant, M. J. Gutmann, J. P. Goff, J.-U. Hoffmann, R. Feyerherm, E. Dudzik, D. Prabhakaran, A. T. Boothroyd, N. Shannon, B. Lake, and P. P. Deen, Nature (London) **445**, 631 (2007).
[29] B. Kang and G. Ceder, Nature (London) **458**, 190 (2009).
[30] L. Wang, F. Zhou, Y. S. Meng, and G. Ceder, Phys. Rev. B **76**, 165435 (2007).